Experimental Study of Reignition Evaluators in Low-Voltage Switching Devices

Dongkyu Shin, Igor O. Golosnoy, and John W. McBride

***Abstract*— The reignition of the arc during the interruption process deteriorates the switching performance of low-voltage switching devices (LVSDs). Avoiding reignition is thus a key goal in the effective design of the quenching chamber. A reliable evaluator of reignition provides the opportunity to predict the switching performance of an LVSD during the design process and to refine the product prior to manufacture and empirical device testing. In this paper, reignition evaluators are investigated through the analysis of interruption test data for several types of LVSDs under the single-phase and three-phase circuit conditions. It is observed that the ratio of the recovery voltage to exit arc voltage, where exit arc voltage is defined as the value of the arc voltage immediately prior to the current zero point, is a reliable evaluator for the prediction of reignition in the switching tests of LVSDs. It is also noted that there are no occurrences of instantaneous reignition where this voltage ratio lies in the range from 1 to −1, and there is a threshold of the voltage ratio at approximately −2, which can distinguish the successful interruption and instantaneous reignition.**

***Index Terms*— Exit arc voltage, low-voltage switching device (LVSD), reignition evaluator, switching performance, voltage ratio.**

I. Introduction

LOW-VOLTAGE switching devices (LVSDs) are widely utilized in power distribution networks to turn ON and OFF circuits and to protect humans and other connected equipment against overload or short-circuit accidents. The quenching chamber of an LVSD is the main volume for switching current and consists of a movable and fixed contact, splitter plate, side plate, magnetic yoke, and vent, as shown in Fig. 1. When the movable contact separates from the fixed contact, an arc is established in the contact gap, which then moves toward the splitter plates by the combination of gas flow and Lorentz forces. After the arc enters the splitter plates, there is an increase in the arc voltage resulting from the multiple anodic and cathodic potential drops associated with the surface interactions with the splitter plates. Ideally, the arc is extinguished at the first current zero moment or sooner in the case of a current-limiting device, however, the arc can reignite after the current zero point.

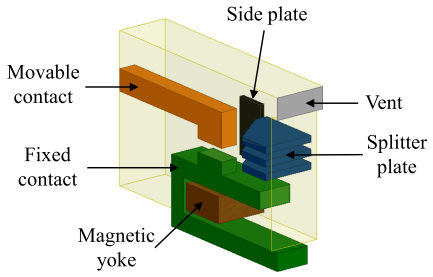

Fig. 1. Half symmetric geometry of a quenching chamber in an LVSD.

The present market trend for LVSDs is toward a more compact product with higher breaking capacity. In order to produce competitive products meeting this demand with low development costs in a short time, it is essential to predict the switching performance of an LVSD and to optimize a product prior to manufacturing a real device. One of the main factors in the deterioration of the switching performance is reignition after the first current zero point. Reignition in an LVSD interruption refers to the failure of the arc interruption at the first current zero point; hence, the current continues its flow after the current zero point. Reignition may lead to longer arcing duration, severe contact erosion, and side-wall damage of LVSDs during the interruption process. Avoiding reignition is therefore crucial when designing a quenching chamber. In practice a reliable evaluator is required to predict the reignition phenomena and to evaluate the switching performance of a particular device prior to empirical testing of real products.

It has been suggested that if the breakdown voltage is greater than the recovery voltage (applied voltage across the breaker at zero current point), there will be a successful interruption without reignition [1], [2]; however, the problem of determining the breakdown voltage of the arc plasma after the current zero point has not been fully addressed due to the changes at the breakdown characteristics of the gas–plasma mixture by complex recombination and cooling processes in the breakers. Some experimental studies have been undertaken regarding the breakdown voltage after the current zero point and evaluators of reignition in LVSDs in order to achieve the improved performance of switching devices. Shea [3] measured the breakdown voltage depending on the vent area of a quenching chamber and reported that

Manuscript received March 2, 2017; revised July 13, 2017, September 26, 2017, and December 6, 2017; accepted February 8, 2018. Recommended for publication by Associate Editor R. Coutu upon evaluation of reviewers' comments. *(Corresponding author: Dongkyu Shin.)*

D. Shin and I. O. Golosnoy are with the School of Electronics and Computer Science, University of Southampton, Southampton SO17 1BJ, U.K. (e-mail: ds7g14@soton.ac.uk).

J. W. McBride is with the Faculty of Engineering and the Environment, University of Southampton, Southampton, SO17 1BJ, U.K., and also with the University of Southampton Malaysia Campus, Malaysia 79200.

Color versions of one or more of the figures in this paper are available online at http://ieeexplore.ieee.org.

Digital Object Identifier 10.1109/TCPMT.2018.2805719

increasing the vent area enhances the breakdown voltage after current interruption. Takahashi and Lindmayer [4] compared the breakdown voltage of the double contacts (U_{Rd}) with that of the single contact (U_{Rs}) and observed that the ratio $U_{\mathrm{Rd}}/U_{\mathrm{Rs}}$ is 1.7–1.8 for Ag alloy contact material, such as AgNi 90/10, AgCdO 90/10, and $AgSnO_2$88/12. Chen *et al.* [5] investigated the recovery characteristics of the breakdown voltage in four different chambers of the magnetic contactor in an attempt to understand the effect of the configuration of the quenching chamber. More complex evaluators have been also suggested. Balestrero *et al.* [6], [7] presented the microscopic evaluators that can forecast reignition by obtaining the arc voltage or current through a sensitive current-measuring device with a signal processing algorithm, for conditions under 10 kA. There were the current decay rate and the change in electric conductivity of the plasma in the microscopic evaluators; however, implementation of these evaluators is not an easy task for a large-scale evaluation campaign. Hauer *et al.* [8], [9] introduced the concept of the exit arc voltage, the arc voltage immediately prior to the current zero point, and proposed that the probability of reignition after the current zero moment is strongly dependent on the exit arc voltage. It was found that the evaluator of the exit arc voltage is a simple tool; however, its reliability has not been rigorously tested. Shin *et al.* [10] proposed an additional evaluator, the ratio of the system voltage to the exit arc voltage at the current zero point, through the switching test results of the miniature circuit breakers (MCBs) and molded case circuit breakers (MCCBs). Chen *et al.* [11] studied the correlation between the arc motion and reignition in magnetic contactors by using optic fiber arc imaging technology and found that the better the arc entry into the splitter plates, the less likely the reignition.

The exit arc voltage could be the simplest evaluator for the industry engineers to evaluate reignition phenomena without the complex calculation of the breakdown voltage; however, it has some limitations regarding the test conditions conducted in previous studies and the accuracy of reignition evaluation. The previous experimental investigation was carried out under a single circuit condition using a single type of MCCB [8], [9]; hence, the reliability of the exit arc voltage needs to be experimentally proved by various kinds of switching conditions. Also, there is no clear threshold value of the exit arc voltage to predict successful interruption. The objective of the work described in this paper is to investigate a more accurate and reliable evaluator for the prediction of reignition based on the switching data of various kinds of test conditions. The proposed evaluator, the voltage ratio, is an extension of the exit arc voltage technique. This paper presents the detailed comparison between the exit arc voltage and voltage ratio as a reignition evaluator. Furthermore, it shows a clear threshold of the voltage ratio between the successful and failed interruption, which can aid in an LVSD design.

II. Experimental Methods and Waveform Analysis

A. Switching Test Circuits and Conditions

The experimental investigation is carried out with 10-, 20-, 55-, and 100-kA test circuits using either MCBs or MCCBs.

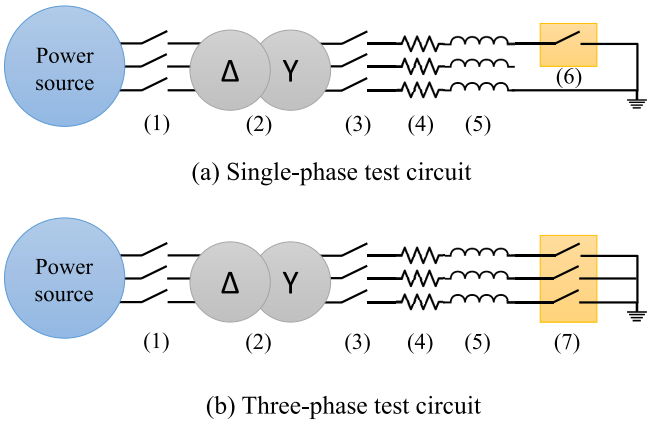

Fig. 2. Test circuit diagrams for a (a) single-phase and (b) three-phase LVSD: (1) back-up circuit breaker, (2) three-phase transformer, (3) making switch, (4) resistor, (5) reactor, (6) single-phase MCB, and (7) three-phase MCB or MCCB.

Fig. 2 shows diagrams of the interruption test circuits for single- and three-phase LVSDs. The short-circuit condition is adjusted by a transformer, resistor, and reactor. Only R and T phases are utilized for the single-phase tests.

A 13.8-kV commercial power line is used as the power source for the 10- and 20-kA switching tests, whereas a short-circuit generator provides the energy for the 55- and 100-kA tests. The current and voltage of each phase are recorded by an oscilloscope (10 MHz, Yokogawa DL750), a passive voltage probe (250 MHz, Tektronix P5100), and a Rogowski current transducer (16 MHz, PEM CWT). No special filters are used to smooth the waveforms. The observed fluctuations in the waveforms are reflections of a physical phenomenon related to the back-and-forward motion of the arc at the splitter plates [12].

Table I shows the test condition of each switching case. A total of 110 interruption tests are conducted with previously unused switching devices under five different test circuits. Table II shows the quenching chamber features of the LVSDs used for given switching tests. When the circuit condition is repeated for the tests on the same LVSD type (for example, the switching cases of test number 1–26 in Table I), the venting condition varies and some components within the quenching chamber are replaced. This includes changing the geometry of the movable and fixed contact, splitter plate, side plate, magnetic yoke, or gassing material. Therefore, there is no identical test condition among 110 switching cases presented in Table I. Testing a variety of circuit conditions and chamber configurations provides the broad switching results for the thorough investigation of reignition evaluators.

There are two types of the interruption operation in the switching tests: the open interruption and close-open interruption. The open interruption represents the switching test where short-circuit current starts to flow through a closed LVSD, and the contacts automatically open due to short-circuit current. The close-open interruption is the switching test where an LVSD manually operates from the open state to the close state while the system voltage is applied across a device, and then the contacts automatically open. The single-phase

TABLE I
SWITCHING TEST CONDITIONS

Number of phase	Voltage [a]	Prospective current	Power Factor [b]	Kind of LVSDs	Test number [c]
1	252 V	10 kA	0.45 [d]	63AF [e] MCB	1 - 26
3	483 V	10 kA	0.45 [d]		27 - 28
		20 kA	0.3	100AF MCCB	29 - 41
				125AF MCCB	42 - 48
				250AF MCCB	49 - 52
				800AF MCCB	53 - 56
		55 kA	0.2	125AF MCCB	57 - 65
				160AF MCCB	66 -67
				250AF MCCB	68 - 69
				400AF MCCB	70 - 73
				800AF MCCB	74 - 78
		100 kA	0.2	160AF MCCB	79 - 86
				250AF MCCB	87 - 88
				400AF MCCB	89 - 91
				630AF MCCB	92 - 99
				800AF MCCB	100 - 110

[a] The voltage value refers to the phase voltage in single-phase tests and line-to-line voltage in three-phase tests.
[b] The power factor is selected according to IEC 60947-2 [13].
[c] The test number corresponds to the switching data in Fig. 6 and 7.
[d] According to IEC 60947-2, the power factor is 0.5 when short-circuit current is 10 kA.
[e] Ampere Frame(AF) represents the frame size rating of the LVSD.

TABLE II
QUENCHING CHAMBER FEATURES OF LVSDS

Kind of LVSDs [a]	Type of chamber [b]	Quantity of splitter plates	Parameters [c]
63AF MCB	Single	13	- Venting condition - Geometry of movable and fixed contact - Geometry of splitter plate - Geometry of side plate - Geometry and kind of gassing material [d]
100AF MCCB	Single	10	- Venting condition - Geometry of splitter plate - Geometry of gassing material
125AF MCCB	Single	10	- Venting condition - Geometry of splitter plate - Geometry of gassing material
160AF MCCB	Double	16	- Venting condition - Geometry of magnetic yoke - Geometry of gassing material
250AF MCCB	Double	16	- Venting condition - Geometry of magnetic yoke [e] - Geometry of side plate [e]
400AF MCCB	Double	18	- Geometry of splitter plate - Geometry of magnetic yoke
630AF MCCB	Double	18	- Geometry of movable contact - Geometry of splitter plate - Geometry of magnetic yoke
800AF MCCB	Double	18	- Geometry of movable contact - Geometry of splitter plate - Geometry of magnetic yoke

[a] Each kind of LVSDs has a different configuration of the quenching chamber. In general, the quantity of splitter plates is larger and the volume of a quenching chamber is bigger as the ampere frame (AF) becomes higher.
[b] There are two types of quenching chambers in LVSDs: one is a single contact chamber and the other is a double contact chamber.
[c] When the circuit condition is fixed for the tests on the same kind of the LVSD (for example, the switching cases of test number 1 – 26 in Table I), several design parameters (the venting condition and the geometry of a movable contact, fixed contact, splitter plate, side plate, magnetic yoke or gassing material) of the quenching chamber are changed.
[d] The polymer can be placed inside the quenching chamber to improve the switching performance. This polymer is called the gassing material.
[e] The side plate and magnetic yoke (shown in Fig. 1) influence the magnetic field in the chamber and they help to increase Lorentz force on the arc.

switching test is conducted through either the open or close-open interruption operation. However, the three-phase test is performed only through the close-open operation in order to obtain an accurate extrapolation of the system voltage at the current zero point. It is difficult to calculate the system voltage at the current zero point by the extrapolation method in a three-phase open interruption test due to distortions observed in the voltage waveforms after switching. The distortions may result from the step voltage applied to the circuit and associated traveling wave reflection at nonmatching impedance points.

B. Waveform Analysis

1) Switching Results: There are three possible switching outcomes: 1) a successful interruption without reignition; 2) a failed interruption with instantaneous reignition; or 3) a failed interruption with delayed reignition. All interruptions with reignition are regarded as failures in this paper. Fig. 3 shows the current and voltage waveforms of a successful interruption and two kinds of reignition in the switching test of LVSDs. In the successful interruption, the arc is extinguished at the first current zero point without reignition [see Fig. 3(a)]. In the case of instantaneous reignition, the arc reignites and the current continues to flow immediately following the current zero point [see Fig. 3(b)]; however, delayed reignition has a pause without current flowing prior to arc reignition [8], [9] [see Fig. 3(c)]. It is believed that instantaneous reignition is related to a high temperature of the arc plasma, which keeps sufficient electrical conductivity of the residual plasma, whereas delayed reignition relies on the dielectric breakdown, which is mainly influenced by the recovery and breakdown voltage. Often, delayed reignition is a consequence of the movable contact's back motion in the quenching chamber of the LVSD.

2) Exit Arc Voltage, Reignition Arc Voltage, and System Voltage at the Current Zero Point: To investigate reignition evaluators, the following parameters are derived from the switching waveforms: 1) the exit arc voltage; 2) reignition arc voltage; and 3) system voltage at the current zero point. The exit arc voltage is now defined as the value of the arc

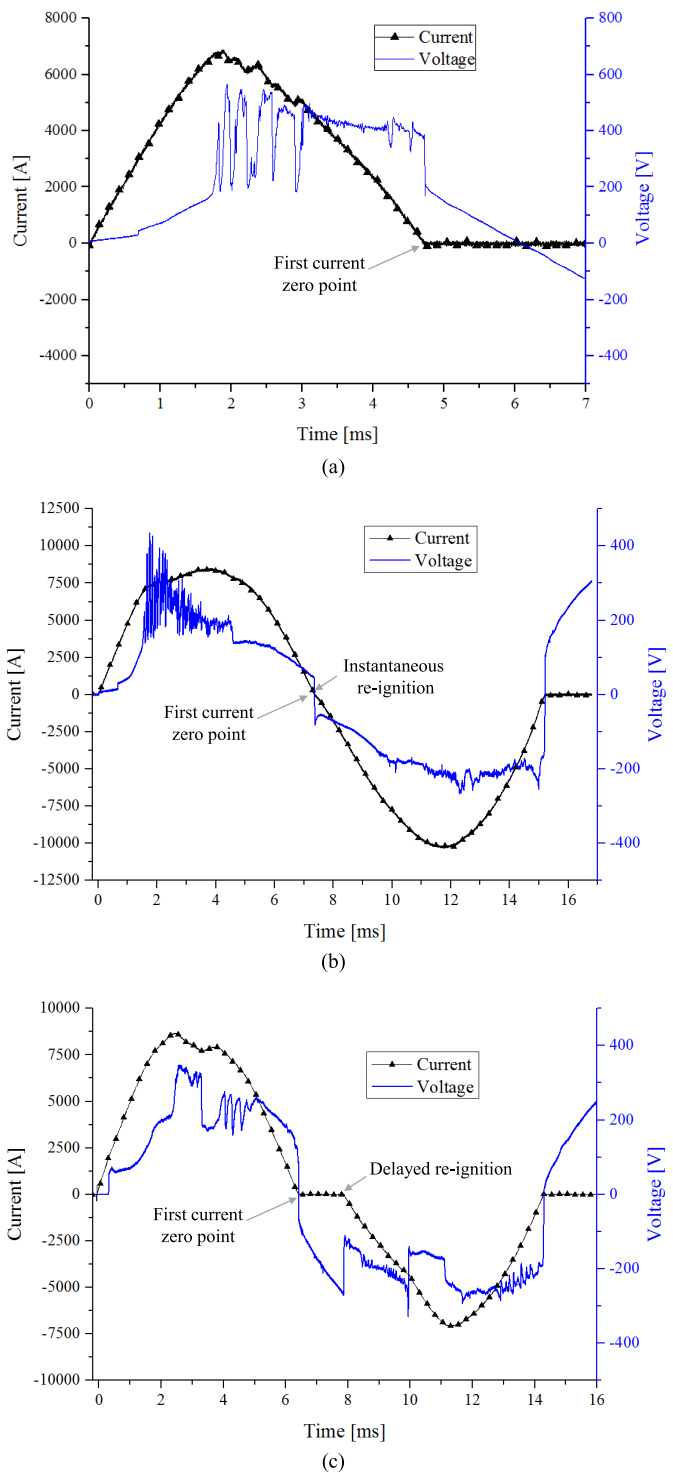

Fig. 3. Current and voltage waveforms of a successful interruption and two kinds of reignition: these are the switching results of single-phase MCBs under 252-V and 10-kA condition. (a) Waveforms of successful interruption: The fluctuations of the arc voltage between 2 and 3 ms are related to the back-and-forward arc motion at the splitter plates [12]. (b) Waveforms of instantaneous reignition. (c) Waveforms of delayed reignition.

voltage 20 μs prior to the current zero point in either successful or failed interruptions, coinciding with the definition provided by Hauer *et al.* [8], [9]. The reignition arc voltage is the value of the arc voltage 20 μs after the current zero point

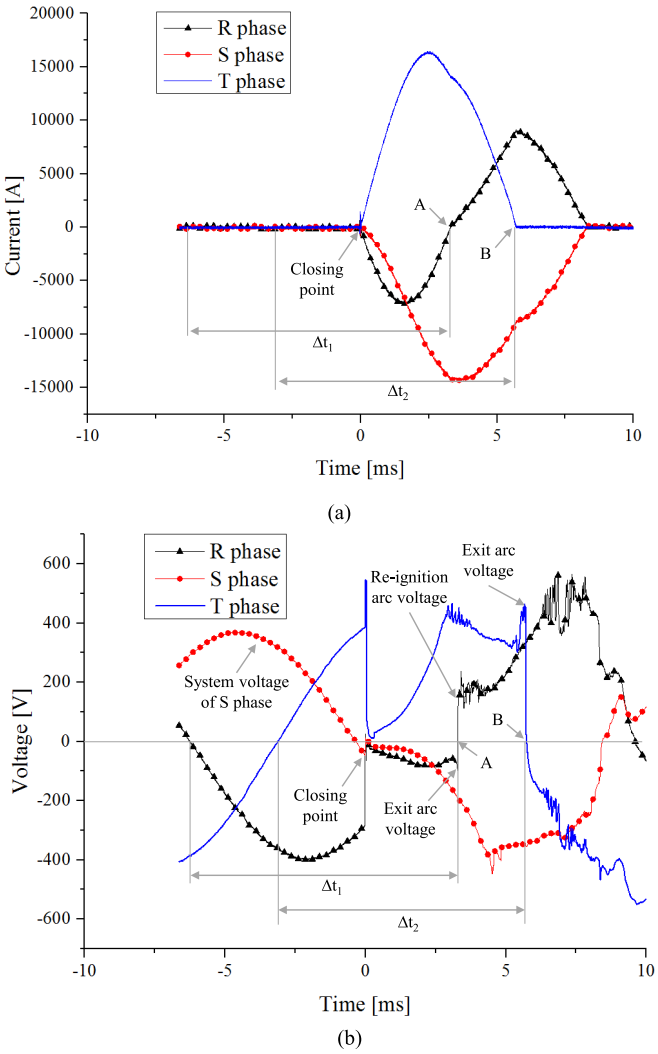

Fig. 4. (a) Current and (b) voltage waveforms of a three-phase MCCB switching test under 483-V and 20-kA condition: A is the first current zero point in R phase, and B is the first current zero point in T phase.

only when instantaneous reignition occurs. The system voltage at the current zero point is the value of the supplied voltage across an LVSD when the arc is extinguished or reignites.

Fig. 4 shows typical current and voltage waveforms during a three-phase interruption process of an MCCB where instantaneous reignition occurs in the R phase and the arc is first extinguished in the T phase. The moving contacts of the device are manually closed to the fixed contacts at 0 ms and instantaneously begin to separate automatically due to the repulsion force caused by short-circuit current. It is observed that the arc voltage rises as the contact gap increases and, after passing the current zero point (A), the arc polarity reverses to match the current polarity in the R phase. After instantaneous reignition, the reignition arc voltage is recorded as a relatively high value when compared with the exit arc voltage, and finally the arc current is interrupted at the first current zero point (B) of the T phase. The exit and reignition arc voltage are directly measured from the arc voltage waveforms. The system voltages at the current zero points (A and B) are

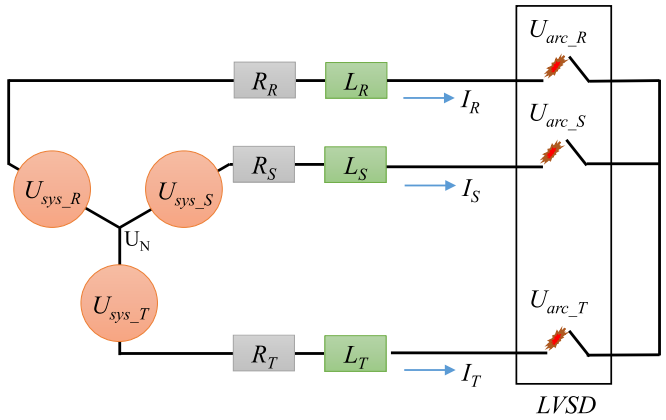

Fig. 5. Equivalent circuit diagram of a three-phase switching test: U_{sys} is the system voltage, I is short-circuit current, U_{arc} is the arc voltage, U_{N} is the voltage at the neutral point, R is the resistance, L is the inductance, and the subscripts (R, S, and T) represent each phase of the circuit.

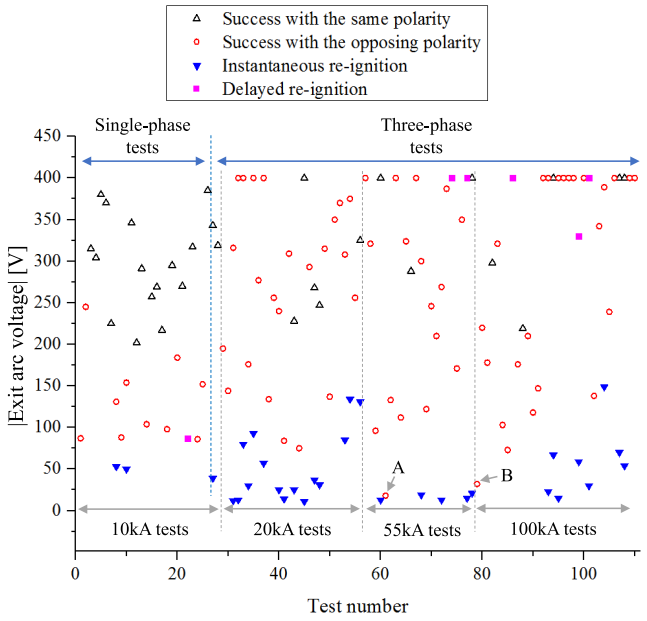

Fig. 6. Reignition occurrences depending on the exit arc voltage: The exit arc voltage is plotted as 400 V if it is greater than 400 V.

obtained through the extrapolation using the time period from the current zero point to the last zero moment of the system voltage prior to the arc ignition (Δt_1 and Δt_2).

In the case of the open interruption, the system voltage at the current zero point is computed by the extrapolation method based on the first zero point of the system voltage after the arc extinction.

If instantaneous reignition occurs, the data of the next current zero event are measured, which is either a successful interruption or delayed reignition.

3) Voltage Ratio: Fig. 5 shows the equivalent circuit diagram of the three-phase switching test, and the circuit equation of the R-phase based on Kirchhoff's voltage law can be expressed as [14]

$$U_{\mathrm{sys\_R}}(t) = I_{\mathrm{R}}(t)R_{\mathrm{R}} + L_{\mathrm{R}}\frac{dI_{\mathrm{R}}(t)}{dt} + U_{\mathrm{arc\_R}}(t) + U_{\mathrm{N}}. \quad (1)$$

We can get the following equations since the three-phase power sources are synchronized:

$$U_{\mathrm{sys\_R}}(t) + U_{\mathrm{sys\_S}}(t) + U_{\mathrm{sys\_T}}(t) = 0 \quad (2)$$

$$I_{\mathrm{R}}(t) + I_{\mathrm{S}}(t) + I_{\mathrm{T}}(t) = 0 \quad (3)$$

$$\frac{dI_{\mathrm{R}}(t)}{dt} + \frac{dI_{\mathrm{S}}(t)}{dt} + \frac{dI_{\mathrm{T}}(t)}{dt} = 0. \quad (4)$$

The voltage at the neutral point in the power source part can be calculated from the following equation by using the three circuit equations of each phase and (2)–(4):

$$U_{\mathrm{N}} = -\frac{U_{\mathrm{arc\_R}}(t) + U_{\mathrm{arc\_S}}(t) + U_{\mathrm{arc\_T}}(t)}{3}. \quad (5)$$

It is assumed that the recovery voltage applied across each phase of the LVSD is composed of the system voltage and the neutral point voltage. Since the arc voltage becomes zero at the current zero point, the recovery voltage across the R phase can be written as

$$U_{\mathrm{rec\_R}} = U_{\mathrm{sys\_R}}(t) + \frac{U_{\mathrm{arcs}}(t) + U_{\mathrm{arc\_T}}(t)}{3}. \quad (6)$$

The voltage ratio is defined as the ratio of the recovery voltage to the exit arc voltage. For the three-phase and single-phase system, the voltage ratio can be formulated, respectively, as

$$\text{Voltage ratio} = \frac{U_{\mathrm{rec}\_j}}{U_{\mathrm{exit}\_j}} \quad (7)$$

$$\text{Voltage ratio} = \frac{U_{\mathrm{sys}}}{U_{\mathrm{exit}}} \quad (8)$$

where U_{exit} is the exit arc voltage and j is the index of the phase. In the single-phase test, only the system voltage is assumed as the recovery voltage.

4) Polarity Between the Recovery Voltage and Exit Arc Voltage: When comparing the polarity of the recovery and exit arc voltage, there are two possible cases: the same polarity or opposing polarities. If there is a strong current-limiting effect and a high exit arc voltage during the interruption process, the current drops to zero prior to the zero point of the system voltage, and the same polarity case is observed.

III. Results and Discussion

The exit arc voltage, proposed by Hauer [8], [9], is the simplest evaluator to predict instantaneous reignition, which is easy to implement in an industrial design scenario. However, this evaluator does not consider the recovery voltage, which is the source of the breakdown (reignition), and its limitation in predicting successful interruption is observed in the switching test data (Fig. 6). First, there are some successful interruption cases where the exit arc voltage is too small to forecast the success, and therefore, a failed interruption is expected according to the exit arc voltage. Second, there is no clear threshold to distinguish a successful and failed interruption in the evaluator of the exit arc voltage. To overcome the limitations of the exit arc voltage as a sole evaluator and

to predict reignition more accurately, the voltage ratio is introduced in this paper, as in (7) and (8).

A. Exit Arc Voltage as an Evaluator

Fig. 6 presents the full data of the correlation between arc reignition occurrence and the absolute value of the exit arc voltage in 10-, 20-, 55-, and 100-kA switching tests. Since each point corresponds to a different test conditions or device designs, a large variation in the exit arc voltage is observed as expected. If the exit arc voltage exceeds 400 V, it is plotted as 400 V. There are 30 successful interruptions with the same polarities between the recovery and exit arc voltage, 74 successful ones with the opposing polarities, 31 instantaneous reignition events, and six delayed reignition events in the switching data. In general, the absolute value of the exit arc voltage is low in the case of instantaneous reignition, whereas a high value is observed in the successful interruption cases. However, there are two limitations in the usage of the exit arc voltage as an evaluator for instantaneous reignition, as presented in Fig. 6. The average value of the exit arc voltage of all instantaneous reignition events is 47 V, but two successful cases (A and B) are marked below this average, which is not explained by the evaluator of the exit arc voltage alone. In addition, there is no clear threshold between successful and failed interruptions.

Except for A and B points, the minimum exit arc voltage in the case of the successful interruption is 73 V, whereas the maximum value in the instantaneous reignition case is 149 V. There are 20 successful cases and 6 instantaneous reignitions in this overlapping region between 73 and 149 V, which are not predicted by the exit arc voltage, accurately.

The delayed reignition phenomena cannot be predicted by the exit arc voltage. This may be attributed to a fault in the LVSD operating mechanism detected during the post-test examination of the device. As an example of the post-test examination, if the movable contact is not locked by the operating mechanism after opening, it can rebound and the contact gap will reduce, causing a failure.

B. Voltage Ratio as an Evaluator

Fig. 7 uses the same test data as Fig. 6, but now shows the dependence of the reignition occurrence on the voltage ratio defined in (7) and (8). Values below a voltage ratio of -3 are plotted as -3. Three groups of the voltage ratio are observed: The first (region 1) is the positive ratio (in the case of the same polarity between the exit and system voltage), the second (region 2) is the range from 0 to -2, and the third (region 3) is less than -2. Omitting the cases of delayed reignition, all switching trials are successful in the range of the positive voltage ratio. There are 74 successful interruptions with the opposing polarity and two instantaneous reignition cases in the second region from 0 to -2 voltage ratio. Only instantaneous reignition events are seen in the range below -2. Particularly, both A and B successful interruptions are predicted by the voltage ratio, which is -0.52 and -1.37, respectively, but not by the exit arc voltage evaluator. Overall, it can be concluded that the voltage ratio is a more detailed and accurate evaluator to forecast the switching performance than the exit arc voltage.

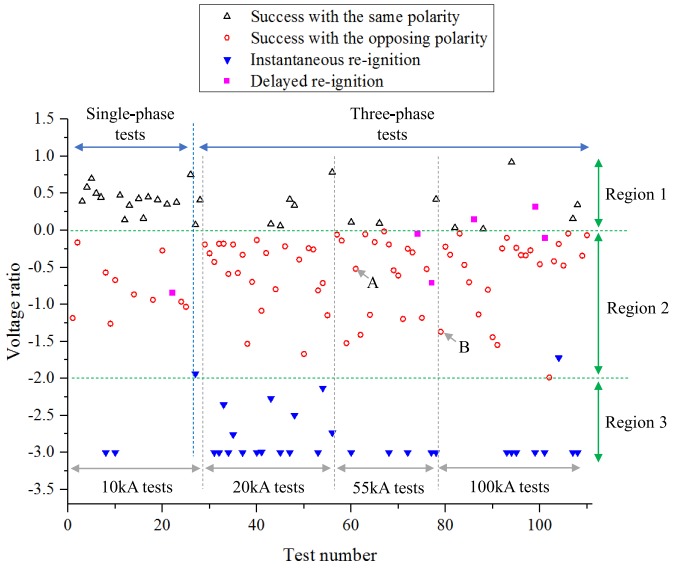

Fig. 7. Reignition occurrences depending on the voltage ratio: the voltage ratio is plotted as -3 if it is lower than -3.

Like the exit arc voltage, the voltage ratio evaluator cannot predict delayed reignition that is associated with the failure of the operating mechanism of the LVSD.

C. Discussion

1) Region of the Positive Voltage Ratio: The successful operation with a positive voltage ratio can be explained by the inconsistency of the circuit equation near the current zero point. As the voltage drop across the external resistive load is negligible, the circuit equation near the current zero point in the single-phase test can be expressed as

$$U_{\mathrm{sys}}(t) - U_{\mathrm{arc}}(t) = L\frac{dI(t)}{dt}. \tag{9}$$

For the three-phase circuit, the voltage between the system voltage and the voltage at the neutral point is required in (9). If instantaneous reignition occurs in the range of the positive voltage ratio with the decreasing current where both system voltage and exit arc voltage are initially positive, the value of the left-hand side in (9) prior to the current zero moment is negative due to a higher arc voltage compared to the system voltage, but it switches to positive immediately after the current zero moment due to a positive system voltage and the inversion of the arc voltage to negative. However, the value of the right-hand side is still negative because the current continues to decrease after the current zero point. It indicates that such situations are not possible and the only solution is an open circuit, i.e., successful interruption.

2) Region of the Negative Voltage Ratio: The situation of the negative voltage ratio can be explained with the aid of the race theory presented by Slepian [1]. Instantaneous reignition occurs in the case of the recovery voltage (which is effectively an open-circuit voltage across the gap in the device) being higher than the breakdown voltage immediately after the current zero point. As the value of the arc voltage is

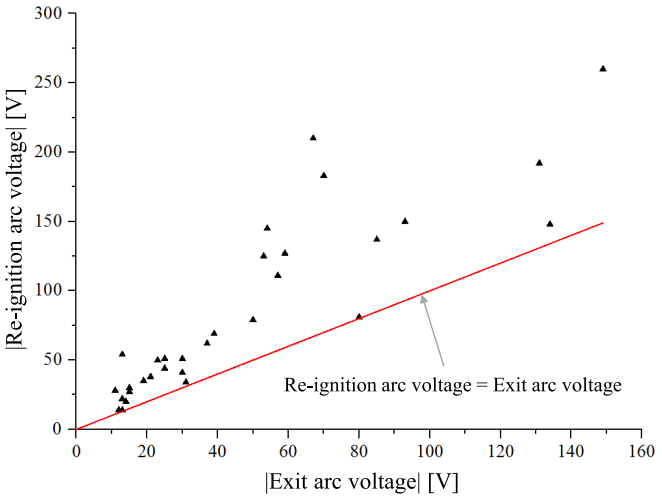

Fig. 8. Relationship between the absolute values of the reignition arc voltage and exit arc voltage: The absolute value of the reignition arc voltage is higher than that of the exit arc voltage in all cases.

determined by the power input required to sustain the arc [2], the breakdown voltage should be greater than the arc voltage.

It is observed from Fig. 8 that the absolute value of the reignition arc voltage (the arc voltage immediately after the current zero point) is greater than that of the exit arc voltage in all instantaneous reignition cases. From this test result, it is apparent that the exit arc voltage has a significant influence on the arc characteristics immediately after the current zero point. Furthermore, Fig. 8 shows that different test conditions lead to very different reignition arc voltages, which in turn indicates that the exit arc voltage itself is probably not the best evaluator.

It is in agreement with the theory that there is no instantaneous reignition in the range from 0 to -1 voltage ratio, i.e., when the breakdown voltage is higher than the recovery voltage. (Note that the breakdown voltage is always higher than the exit arc voltage due to cooling effects.) In practice, the threshold between successful and unsuccessful interruptions is observed at more relaxed conditions, when the voltage ratio is approximately -2 (see Fig. 7). There are two possible explanations for the observed threshold. The increase in the breakdown voltage due to plasma cooling and reduction in plasma conductivity is possible; therefore, a higher-than-the-exit-arc voltage is needed to support a colder arc. The other explanation can be a switching of cathodic and anodic sheaths over the splitter plate surfaces. This switch takes place just before reignition when the sufficient recovery voltage is applied to: 1) compensate the voltage drop (which corresponds to the exit arc voltage) in the existing sheaths allowing electrons and ions to move in the opposite direction; and 2) to create an additional voltage drop with opposite polarities accelerating electrons and ions for the ions generation at the anodic sheath and the electron emission from the cathode by ions bombardment. The magnitude of this additional voltage is equal to the exit arc voltage if we assume that the latter one is almost all due to the surface sheaths.

There are rare cases when reignition occurs at the ratio above -2. We believe that these cases correspond to situations when the arc is attached at the edges of some splitter plates prior to the current zero point and the arc reignites directly through an air gap skipping the edges. This reignition does not require the sheath switch as the arc is established through the hot gas region in front of the splitter plates without creating an additional voltage drop in the cathode and anode sheath. In this case, the breakdown voltage can be less than 200% of the exit arc voltage, however, always greater than 100% of the exit arc voltage. The modeling can select the LVSD design to push the arc further toward splitter plates, and this would allow to consider the relaxed reignition criterion, the voltage ratio > -2.

IV. Conclusion

In this paper, an experimental investigation has been carried out regarding reignition evaluators that can predict the switching performance of LVSDs prior to empirical laboratory testing of real products. The following conclusions can be drawn.

1) The voltage ratio (which is defined as the ratio of the recovery voltage to the exit arc voltage) is a reliable evaluator and provides more information than the exit arc voltage.
2) Instantaneous reignition does not occur when the voltage ratio is positive or it lies in the range from 0 to -1. It can be used as a "strict" global evaluator to predict the switching performance of the LVSD. Also, there is an experimentally observed "soft" threshold of the voltage ratio at approximately -2, which distinguishes most of the successful interruptions from instantaneous reignitions. The rare cases of reignition when the ratio lies in the range from -1 to -2 are attributed to the arc attachment at the edges of splitter plates and reignition directly through an air gap without the sheath voltage.
3) Delayed reignition cannot be predicted by using either the exit arc voltage or voltage ratio; however, it was diagnosed with the result of failure in the LVSD operating mechanism. It should be the subject of mechanical design improvement, rather than optimization of electrical arc dynamics.

References

[1] J. Slepian, "Extinction of an A-C. Arc," *Trans. Amer. Inst. Electr. Engineers*, vol. 47, no. 4, pp. 1398–1407, Oct. 1928.
[2] P. G. Slade, *Electrical Contacts: Principles and Applications*. New York, NY, USA: CRC Press, 2014, pp. 553–616.
[3] J. J. Shea, "Dielectric recovery characteristics of a high current arcing gap," *IEEE Trans. Compon. Packag. Technol.*, vol. 25, no. 3, pp. 402–408, Sep. 2002.
[4] A. Takahashi and M. Lindmayer, "Reignition voltage of arcs on double-break contacts," *IEEE Trans. Compon., Hybrids, Manuf. Technol.*, vol. CHMT-9, no. 1, pp. 35–39, Mar. 1986.
[5] D. Chen, X. Li, and R. Dai, "Measurement of the dielectric recovery strength and reignition of AC contactors," *IEICE Trans. Electron.*, vol. E88-C, no. 8, pp. 1641–1646, Aug. 2005.
[6] A. Balestrero, L. Ghezzi, M. Popov, and L. V. D. Sluis, "Current interruption in low-voltage circuit breakers," *IEEE Trans. Power Del.*, vol. 25, no. 1, pp. 206–211, Jan. 2010.
[7] L. Ghezzi and A. Balestrero, "Modeling and simulation of low voltage arcs," Ph.D. dissertation, Dept. Elect. Power Eng., Delft Univ. Technol., Delft, The Netherland, 2010.
[8] W. Hauer and X. Zhou, "Re-ignition and post arc current phenomena in low voltage circuit breaker," in *Proc. ICEC*, Jun. 2014, pp. 398–403.

[9] W. Hauer, "Re–ignition phenomena in low–voltage circuit breakers," Ph.D. dissertation, Dept. Phys., Vienna Univ. Technol., Austria, Wien, Austria, 2012.
[10] D. Shin, I. O. Golosnoy, and J. W. Mcbride, "Arc modelling for switching performance evaluation in low-voltage switching devices," in *Proc. ICEC*, 2016, pp. 41–45.
[11] D. Chen, R. Dai, and X. Li, "Experimental investigation on the arc motion with different configurations of quenching chamber in AC contactor," *IEICE Trans. Electron.*, vol. E89-C, no. 8, pp. 1201–1205, Aug. 2006.
[12] J. W. McBride, D. Shin, and T. Bull, "A study of the motion of high current arcs in splitter plates using an arc imaging system," in *Proc. ICEC*, 2016, pp. 175–180.
[13] *Low-Voltage Switchgear and Controlgear—Part 2: Circuit Breakers, International Electrotechnical Commission, Edition 4.0*, IEC Standard 60947-2, 2006.
[14] T. Onchi, M. Isozaki, and M. Wada, "Current limiting simulation for low voltage circuit breaker," in *Proc. IECON*, Nov. 2003, pp. 631–636.

Dongkyu Shin received the B.Eng. degree in electrical engineering from Hanyang University, Seoul, South Korea, in 2004, and the M.Eng. degree in electrical engineering from Seoul National University, Seoul, in 2006. He is currently pursuing the Ph.D. degree with the Electronics and Electrical Engineering Research Group, University of Southampton, Southampton, U.K.

Igor O. Golosnoy received the M.Sc. degree in applied mathematics and physics from the Moscow Institute of Physics and Technology, Moscow, Russia, in 1992, and the Ph.D. degree in mathematics and physics from the Institute for Mathematical Modelling, Moscow, in 1995.

He is an Associate Professor at the Electronics and Electrical Engineering Research Group, Faculty of Physical Sciences and Engineering, University of Southampton, Southampton, U.K. His current research interests include numerical modeling of various coupled electrical, thermal, and mechanical phenomena in gas discharges and optical emission spectroscopy of plasmas.

John W. McBride was the Associate Dean of Research with the Faculty of Engineering and the Environment, and also the Chair of the Electro-Mechanical Research Group, University of Southampton, Southampton, U.K. He is currently the CEO of the University of Southampton–Malaysia Campus, Malaysia, and also a member of the Electromechanical Research Group with the University of Southampton, Southampton. He is an Expert in electrical contact physics and surface characterization. He has authored over 200 papers, and holds three patents.